Apoptosis (2014) 19:542–553
DOI 10.1007/s10495-013-0947-y

ORIGINAL PAPER

A monocarbonyl analogue of curcumin, 1,5-bis(3-hydroxyphenyl)-1,4-pentadiene-3-one (Ca 37), exhibits potent growth suppressive activity and enhances the inhibitory effect of curcumin on human prostate cancer cells

Cheng Luo · Yan Li · Bo Zhou · Liang Yang · Hua Li · Zhihui Feng · Yuan Li · Jiangang Long · Jiankang Liu

Published online: 3 December 2013

Abstract Prostate carcinoma is one of the leading causes of cancer-related morbidity and mortality in males in western countries. Curcumin exhibits growth-suppressive activity against several cancers, including prostate cancer, but it has poor bioavailability. The purpose of this study was to evaluate the anticancer potency and mechanism of a curcumin analogue, 1,5-bis(3-hydroxyphenyl)-1,4-pentadiene-3-one (Ca 37), in human prostate cancer. Studies were performed in established human prostate cancer cell lines (PC-3 and DU145) as well as in a murine xenograft tumor (PC-3) model. Ca 37 presented a preferential suppression capacity against growth and migration toward prostate cancer cells compared with curcumin. Ca 37 impaired the bioenergetics system, promoted cell cycle arrest and apoptosis activation in PC-3 cells. In addition, 0.5 μmol (6.65 mg/kg body weight) of Ca 37 significantly inhibited the growth of the prostate xenografted tumors, whereas 6 μmol (110 mg/kg body weight) of curcumin had little effect. Furthermore, a combination of Ca 37 and curcumin resulted in enhanced antitumor activity in prostate cancer cells. *N*-Acetylcysteine abrogated both reactive oxygen species (ROS) production and viability loss induced by Ca 37 but partially prevented growth inhibition in PC-3 cells treated with curcumin alone, or a combination with Ca 37. The data indicate that induction of ROS plays a vital role in the growth inhibitory effect of Ca 37 in PC-3 cells. This study suggests that Ca 37, alone or in combination with curcumin, may be a promising anticancer agent for prostate cancer therapy.

Keywords Curcumin analogue Ca 37 · Prostate cancer · Reactive oxygen species · Tumor xenograft

Abbreviations

CI	Combination index
Complex I	NADH–CoQ oxidoreductase
Complex II	Succinate–CoQ oxidoreductase
Complex III	CoQ–cytochrome *c* reductase
Complex IV	Cytochrome *c* oxidase
DCIP	2,6-Dichlorobenzenone–indophenol
DMSO	Dimethyl sulfoxide
FBS	Fetal bovine serum
ROS	Reactive oxygen species
GSH	Reduced glutathione
H_2DCFDA	2′,7′-Dichlorodihydrofluorescein diacetate
INT	2-(*p*-iodophenyl)-3(*p*-nitrophenyl)-5-phenyl tetrazolium chloride
α-KGDH	α-Ketoglutarate dehydrogenase complex
LA	Lactic acid
LDH	Lactate dehydrogenase
MDH	Malate dehydrogenase
NAC	*N*-Acetylcysteine

C. Luo · L. Yang · H. Li · Z. Feng · Y. Li · J. Long · J. Liu (✉)
Center for Mitochondrial Biology and Medicine, The Key Laboratory of Biomedical Information Engineering of Ministry of Education, School of Life Science and Technology and Frontier Institute of Life Science, FIST, Xi'an Jiaotong University, Xi'an 710049, China
e-mail: j.liu@mail.xjtu.edu.cn

C. Luo
e-mail: luoke123@gmail.com

Y. Li
Center for Bioinformatics, The Key Laboratory of Biomedical Information Engineering of Ministry of Education, School of Life Science and Technology, Xi'an Jiaotong University, Xi'an 710049, China

B. Zhou
State Key Laboratory of Applied Organic Chemistry, Lanzhou University, Lanzhou 730000, China

NBT	Nitroblue tetrazolium
PARP	Poly(ADP-ribose) polymerase
PI	Propidium iodide
PMS	Phenazine methosulfate
RNase A	Ribonuclease A

Introduction

Prostate cancer is the most frequently diagnosed cancer and the second-leading cause of cancer death among men in the United States. According to a cancer statistical report from the American Cancer Society, there will be approximately 241,740 new cases and 28,170 deaths from prostate cancer occurring in the United States in 2012 [1]. Curcumin, a polyphenolic molecule extracted from turmeric, exhibits promising chemopreventive activity against prostate cancer through anti-proliferation and pro-apoptosis activity, prevention of cell motility and metastasis, regulation of the inflammatory response and down-regulation of the androgen receptors and co-factors [2].

Many cancer cells are resistant to chemotherapy due to deregulated apoptosis. The evaluation of the ability to overcome the resistance of tumor cells towards apoptosis, i.e., apoptosis activation, is a routine way to screen chemotherapy drugs. Apoptosis can be divided into two pathways: the intrinsic pathway (signaling involving the mitochondria) and the extrinsic pathway (signaling through death receptors on the cell surface). Pro-apoptosis proteins of the Bcl-2 family, sharing homology in the Bcl-2 homology regions (BH1–BH3) with conserved sequence motifs, initiate the mitochondrial pathway, leading to cytochrome *c* release and then the activation of caspases [3]. The mitochondria are intracellular power houses and a major source of reactive oxygen species (ROS), including superoxide anion radicals, hydroxyl radicals, and hydrogen peroxide (H_2O_2). ROS are active mediators in the regulation of cell dysfunction and death at different levels via induction of protein carbonylation, lipid peroxidation and DNA damage [4]. In curcumin-treated prostate cancer cells, there is a decrease in anti-apoptosis proteins Bcl-2 and Bcl-xL expression, an increase in the pro-apoptosis proteins Bax and Bak, and a translocation of Bax to the mitochondria. ROS generation, cytochrome *c* release and caspase-3 activation are involved in the induction of apoptosis by curcumin [5]. However, a study by Hilchie et al. [6] suggested that the cytotoxic effect of curcumin did not involve ROS generation in PC-3 cells. The researchers compared apoptosis suppression and the ROS scavenging effects of the exogenous antioxidants, including reduced glutathione (GSH), *N*-Acetylcysteine (NAC), ascorbic acid, and ebselen.

However, the poor water solubility and bioavailability of curcumin severely curtails its anti-cancer capacity [7]. Many structural analogues of curcumin have been synthesized to improve its bioavailability [8]. However, many analogues are very expensive for researches or clinic trials, i.e. EF-24 (E8409-5 mg, US$ 69.30, sigma) and FLLL31 (F9057-5 mg, US$ 88.50, sigma). Derivatives with low costs and favorable anti-cancer effects should be developed to benefit the general public. 1,5-bis(3-hydroxyphenyl)-1,4-pentadiene-3-one, a monocarbonyl analogue of curcumin, named Ca 37 herein, was chosen to evaluate its anticancer potency and mechanism against human prostate cancer for its low-cost synthesis. We found that Ca 37 exerts a preferential toxicity toward prostate cancer cells which is dependent on ROS induction, similar to that of other curcumin analogues [9–11].

Materials and methods

Materials

N-Acetyl-cysteine (NAC), CoQ1, crystal violet, decylubiquinone, curcumin, 2-(*p*-iodophenyl)-3(*p*-nitrophenyl)-5-phenyl tetrazolium chloride (INT), dimethyl sulfoxide (DMSO), cisplatin, doxorubicin, 2,6-dichlorobenzenone-indophenol (DCIP), 3-hydroxy-benzaldehyde, glucose-6-phosphate dehydrogenase, CoASH, thiamine pyrophosphate, propidium iodide (PI), phenazine methosulfate (PMS), and an anti-actin primary antibody were obtained from Sigma (St. Louis, MO). RPMI-1640 medium, penicillin, streptomycin, 2′,7′-dichlorodihydrofluorescein diacetate (H_2DCFDA) and trypsin were purchased from Invitrogen (Carlsbad, CA). Primary antibodies for Bax, Bak, Bad, Bcl-xL, Bcl-2, and poly(ADP-ribose) polymerase (PARP) were obtained from Cell Signaling Technology, Inc. (Beverly, MA). Cyclin A, B1, D1, and E were obtained from Santa Cruz Biotechnology (Santa Cruz, CA). Secondary HRP conjugated anti-mouse/rabbit antibodies were purchased from Jackson ImmunoResearch Laboratories, Inc. (West Grove, PA). Ribonuclease A (RNase A) was obtained from Takara Biotechnology (Dalian) Co., Ltd. (Dalian, Liaoning, China). Fetal bovine serum (FBS) was obtained from PAA Laboratories GmbH (Linz, Austria). Hoechst 33342 and cell lysis buffer were obtained from Beyotime Biotechnology (Haimen, Jiangsu, China). Lactate dehydrogenase (LDH) activity and lactic acid (LA) content kits were obtained from the Nanjing Jiancheng Bioengineering Institute (Nanjing, Jiangsu, China).

Synthesis of curcumin analogue Ca 37

Ca 37 was synthesized based on previously described methods [12, 13]. Briefly, aqueous NaOH (20 % (wt),

15 mL, 75 mmol) was added dropwise to a vigorously stirred solution of 3-hydroxy-benzaldehyde (51 mmol) and ketone (25 mmol) in absolute ethanol (8 mL). The reaction proceeded under stirring at room temperature for 48 h, distilled water (40 mL) was added, and the solution was neutralized by HCl. The yellow precipitate was filtered off, washed with distilled water and dried under a vacuum. The resulting product was directly charged onto a silica gel column and eluted with a mixture of ethyl acetate/petroleum to obtain the pure product: a yellow solid; yield: 13.7 %; mp 202–204 °C; ^{1}H NMR (400 MHz, $(CD_3)_2CO$), δ 8.57 (s, 2 H, –OH), 7.72 (d, $J = 16.0$ Hz, 2 H), 7.20–7.30 (m, 8 H), 6.93 (ddd, $J = 7.6$, 2.4, 1.2 Hz, 2 H); ^{13}C NMR (100 MHz, $(CD_3)_2CO$), δ 189.0, 158.8, 143.6, 137.5, 130.9, 126.6, 120.9, 118.5, 115.7; EIMS, *m/z* 266 $[M]^+$.

The purity of Ca 37 was determined to be 99.87 % by HPLC. HPLC analysis was performed using a Waters 600 instrument with photodiode array detector, and a Symmetry Shield™ RP_{18} (3.9 × 150 mm, 5 μm particle size, Waters) with a mixture of isopropanol/*n*-hexane (5:95, v/v) as an eluent. The flow rate was set at 0.5 mL/min.

Cell culture

Human androgen-independent prostate cancer PC-3 (from Chinese Academy of Sciences Committee Type Culture Collection Cell Bank/CAS Shanghai Institutes for Biologic Sciences Cell Resource Center) and DU145 (from the cell bank of the Kunming Institute of Zoology, Chinese Academy of Sciences) cells were maintained at 37 °C with 5 % CO_2 in RPMI 1640 medium containing 10 % FBS, 100 units/mL penicillin and 100 μg/mL streptomycin in a humidified incubator (Thermo Fisher Scientific, Inc., Waltham, MA).

Cell viability/cytotoxicity assay

A crystal violet-based staining assay was used to assess the cytotoxicity of curcumin and Ca 37 [14]. After treatment with the compounds, the cells were fixed with 4 % paraformaldehyde and stained with 0.1 % crystal violet at room temperature, and then excess stain was washed away. The crystal violet in stained cells was dissolved in 30 % acetic acid, and the absorbance was recorded with a microplate spectrophotometer (Thermo Scientific Multiskan™ Spectrum) at 570 nm.

Determination of intracellular reactive oxygen species (ROS)

Intracellular ROS were measured by 2′,7′-dichlorodihydrofluorescein diacetate (H_2DCFDA), which is non-fluorescent unless oxidized within the cell [15]. After staining,

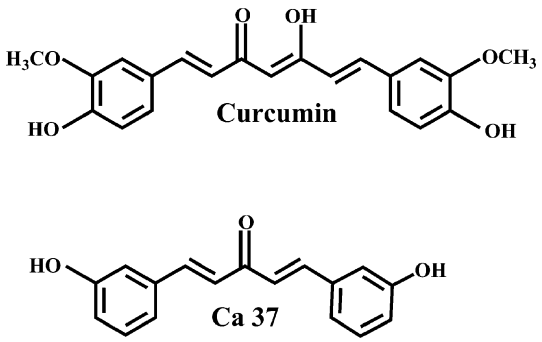

Fig. 1 Chemical structure diagram of curcumin and its analogue Ca 37

the cells were lysed with buffer (10 mmol/L Tris, 150 mmol/L NaCl, 0.1 mmol/L EDTA, 0.5 % Triton X-100, pH 7.5), centrifuged at 13,000*g* for 10 min, and then the supernatant was collected. The fluorescence intensity of the supernatant was recorded with a Thermo Scientific Fluoroskan™ Ascent FL at 485 nm excitation and 535 nm emission and normalized by cellular protein content.

Chromatin condensation

The cells were fixed with 4 % paraformaldehyde, followed by staining with Hoechst 33342 (Beyotime Biotechnology, Jiangsu, China). The fluorescent photographs of chromatin condensation were taken with a fluorescence microscope (Olympus IX71).

Cell cycle analysis

The cells were fixed with 75 % ethanol in −20 °C, followed by staining with PI solution (0.1 % Triton-100, 200 μg/mL RNase A, 20 μg/mL PI). The analysis of cell cycle phases was performed using a BD FACSCanto™ Flow Cytometer according to manufacturer's instructions.

Mitochondrial respiratory chain complex and citric acid cycle enzyme activity

The mitochondria in PC-3 cells were isolated with a differential centrifugation method at 4 °C as follows, similar to our previous work [16]. After swelling in ice-cold RSB (a hypotonic buffer that causes tissue culture cells to swell, 10 mmol/L NaCl, 1.5 mmol/L $MgCl_2$, 10 mmol/L Tris–HCl, pH 7.5) for 15 min, the cells were homogenized with several strokes of a small-clearance pestle in media (210 mmol/L mannitol, 70 mmol/L sucrose, 5 mmol/L Tris–HCl, 1 mmol/L EDTA, pH 7.5) in a 2 mL Dounce homogenizer. The homogenate was centrifuged at 1,300*g* for

5 min, the supernatant was collected and centrifuged at 17,000*g* for 15 min to obtain mitochondrial particles. The mitochondrial protein concentrations were determined using a BCA™ Protein Assay kit (Thermo Scientific). The mitochondria were stored at −80 °C before assayed.

NADH–CoQ oxidoreductase (Complex I) activity was assessed in a reaction mixture (50 mmol/L Tris–HCl, pH 8.1, 0.05 mmol/L DCIP, 0.35 % BSA, 1 μmol/L antimycin A, 0.2 mmol/L NaN_3, 0.05 mmol/L coenzyme Q1, 200 μmol/L NADH), followed by scanning at 600 nm for 2 min at 30 °C [17].

Succinate–CoQ oxidoreductase (Complex II) was assessed in a reaction mixture (50 mmol/L potassium phosphate buffer pH 7.8, 0.05 mmol/L DCIP, 2 mmol/L EDTA, 0.1 % BSA, 3 μmol/L rotenone, 1 μmol/L antimycin A, 0.2 mmol/L NaN_3, 0.2 mmol/L ATP, 0.05 mmol/L CoQ1, 10 mmol/L succinate), followed by scanning at 600 nm for 2 min at 30 °C [18].

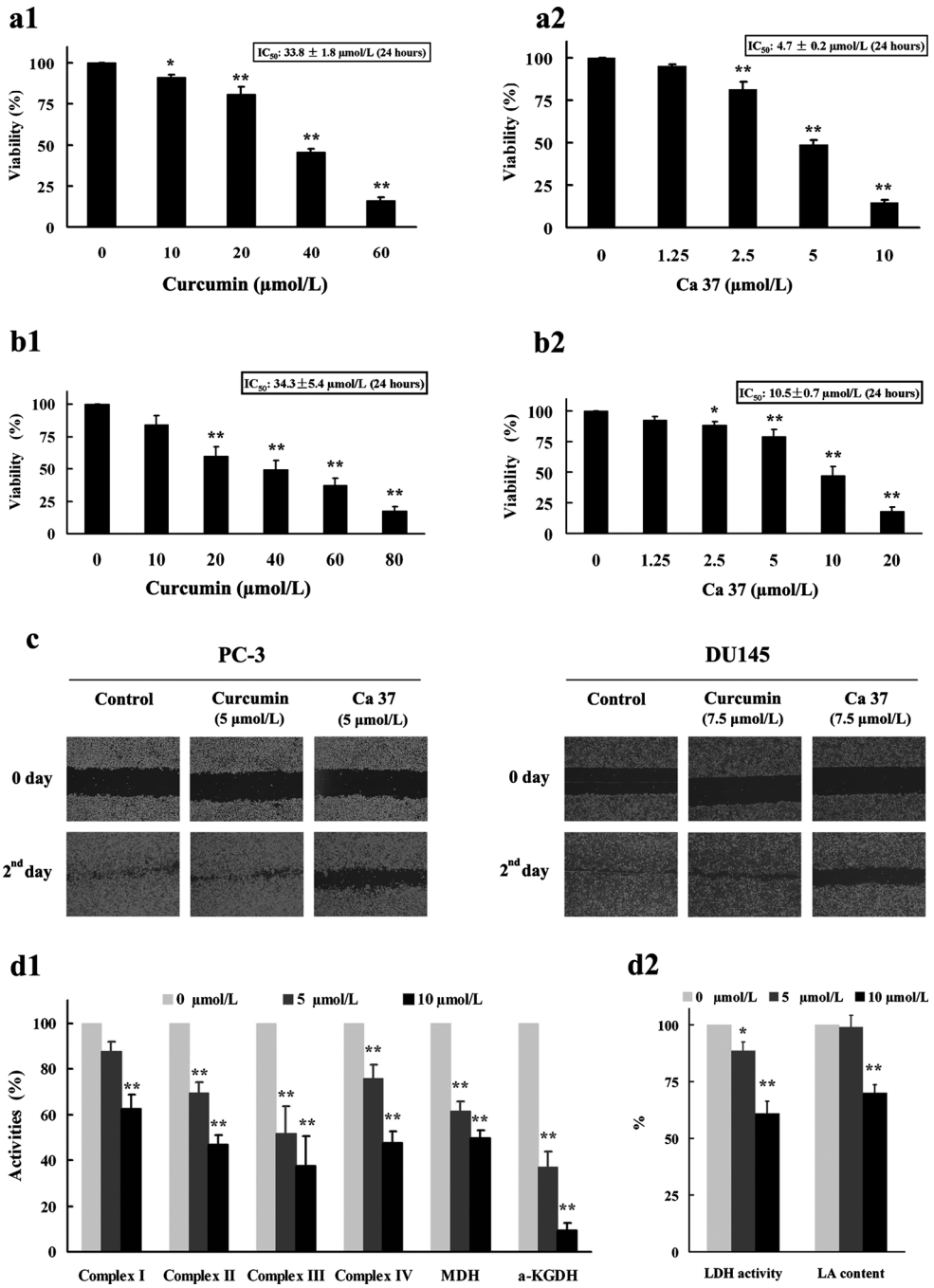

Fig. 2 Ca 37 exhibits potential inhibitory effect against prostate cancer cells. The viabilities of PC-3 cells (**a**) and DU145 cells (**b**) treated with the indicated concentrations of curcumin (**a1**, **b1**) or Ca 37 (**a2**, **b2**); **c** wound healing assay of PC-3 cells and DU145 cells; **d1** the activities of respiration chain complex enzymes (Complex I to Complex IV) and citric acid cycle enzymes (MDH and α-KGDH) in Ca 37-treated PC-3 cells; **d2** the LDH activity and LA content in Ca 37-treated PC-3 cells; **e1** representative images and **e2** quantitative data of cell cycle arrest in 10 μmol/L Ca 37-treated PC-3 cells; **f1** western blot of Bcl-2 family proteins and poly(ADP-ribose) polymerase (PARP) in 10 μmol/L Ca 37-treated PC-3 cells; **f2** the semi-quantified statistics for the western blot normalized with β-actin; **g** chromatin condensation in Ca 37-treated PC-3 cells. $^{*}p < 0.05$, $^{**}p < 0.01$ vs. non-treated control group (vehicle group). All data were from at least 3 independent repeat experiments

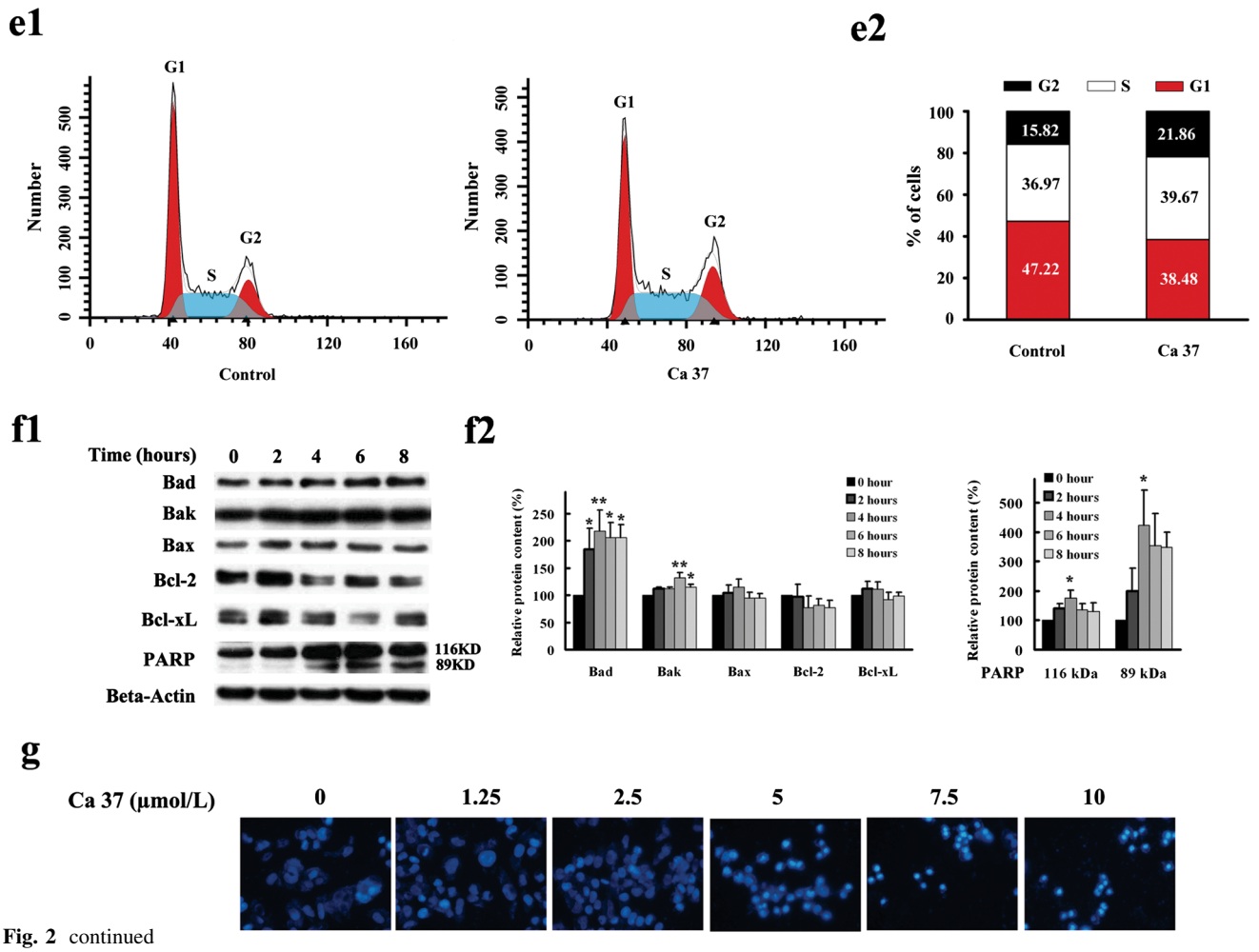

Fig. 2 continued

CoQ–cytochrome *c* reductase (Complex III) was assessed in a reaction mixture (50 mmol/L Tris–HCl pH 7.8, 0.2 mmol/L NaN_3, 0.05 % Tween-20, 0.01 % BSA, 0.05 mmol/L cytochrome *c*, 0.05 mmol/L decylubiquinol), followed by scanning at 550 nm for 2 min at 30 °C [19].

Cytochrome *c* oxidase (Complex IV) was measured in a reaction mixture (50 mmol/L potassium phosphate buffer pH 7.0, 0.1 % BSA, 0.2 % Tween-20, 0.05 mmol/L reduced cytochrome *c*), followed by scanning at 550 nm for 2 min at 30 °C [20].

α-Ketoglutarate dehydrogenase complex (α-KGDH) was assayed in a reaction mixture (35 mmol/L potassium phosphate buffer pH 7.25, 2 mmol/L NaN_3, 0.5 mmol/L EDTA, 2.5 μmol/L rotenone, 5 mmol/L $MgCl_2$, 0.5 mmol/L NAD^+, 0.2 mmol/L thiamine pyrophosphate, 2 mmol/L α-ketoglutarate, 0.04 mmol/L CoASH), followed by scanning at 340 nm for 2 min at 30 °C [21].

Malate dehydrogenase (MDH) activity was assayed in a reaction mixture (15 mmol/L malate, 3 μmol/L rotenone, 0.1 % BSA, 0.5 mmol/L NAD^+, 0.6 mmol/L INT, 0.2 mmol/L PMS, 50 mmol/L potassium phosphate buffer pH 9), followed by scanning at 500 nm for 2 min at 30 °C [16].

Lactate dehydrogenase (LDH) activity and lactic acid (LA) content assessment

Lactate dehydrogenase activity was assessed with a colorimetric method using a commercial kit (Nanjing Jiancheng Bioengineering Institute, Nanjing, Jiangsu, China). According to the manufacturer's instructions, the resulting pyruvate was obtained from lactic acid via lactate dehydrogenase-mediated conversion of 2,4-dinitrophenylhydrazine into a visible brownish red hydrazone in alkaline solutions, and the absorbance of the hydrazone was recorded with a microplate spectrophotometer (Thermo Scientific Multiskan Spectrum) at 440 nm.

Lactic acid content was measured by following NADH production by coupling it to the reduction of nitroblue tetrazolium (NBT) via the intermediate electron carrier phenazine methosulfate (PMS) using a commercial kit (Nanjing Jiancheng Bioengineering Institute, Nanjing, Jiangsu, China). The absorbance of NBT formazan was recorded with a microplate spectrophotometer (Thermo Scientific Multiskan Spectrum) at 530 nm.

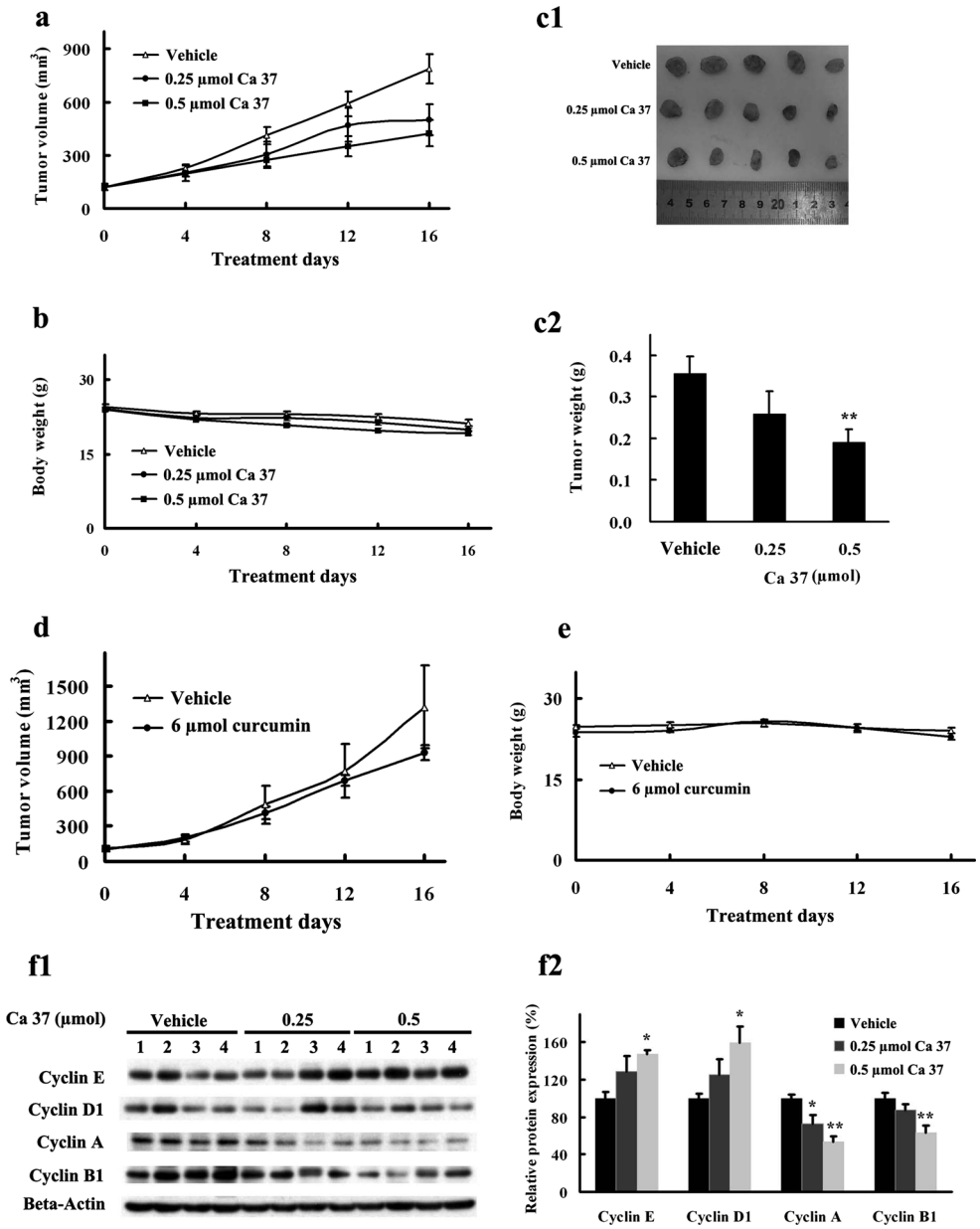

Fig. 3 Ca 37 suppresses prostate cancer tumor xenograft growth in vivo. The tumor volumes (**a**) and mice body weights (**b**) of Ca 37-treated nude mice; the photographs (**c1**) and weights (**c2**) of the tumors from the Ca 37-treated nude mice; the tumor volumes (**d**) and mice body weights (**e**) of curcumin-treated nude mice; **f1** western blot of cell cycle regulation proteins from protein extracts of tumors from the Ca 37-treated nude mice; **f2** the semi-quantified statistics for the western blot (**f1**) normalized with β-actin. $*p < 0.05$, $**p < 0.01$ vs. vehicle group. All data were from at least three independent repeat experiments

Wound healing migration assay

The wound healing assay is a simple method to study directional cell migration in vitro. Cells were plated in a 12-well plate and grown to confluence. A wound was created by dragging a 200 μL pipette tip across the surface of a monolayer culture, and the cellular debris was washed out with PBS. The cells were treated with curcumin or Ca 37 for 2 days, during which time vehicle treatment cells always grew to convergence across the wound, and then images were taken.

In vivo PC-3 tumor xenograft model

Five-week-old male athymic nude mice (BALB/c-nu/nu) were obtained from the Xi'an Jiaotong University College of Medicine Laboratory Animal Center (Xi'an, Shannxi, China). The animal care and treatments were performed in accordance with the animal experimentation guidelines of Xi'an Jiaotong University. All mice were maintained with ad libitum water and sterilized standard mouse chow in sterile filter-capped microisolator cages on a 12 h light/dark cycle in the same animal center. Prostate cancer PC-3 cells were suspended in RPMI 1640 (1×10^7/100 μL/mouse) and injected s.c. into the right flank of the mice. When the injected tumor cells grew to a size of approximately 100 mm^3, the tumor-bearing mice were then divided randomly into treatment groups (five mice per group). The mice received an i.p. injection of DMSO vehicle, 0.25 μmol Ca 37 (3.33 mg/kg body weight), 0.5 μmol Ca 37 (6.65 mg/kg body weight), or 6 μmol curcumin

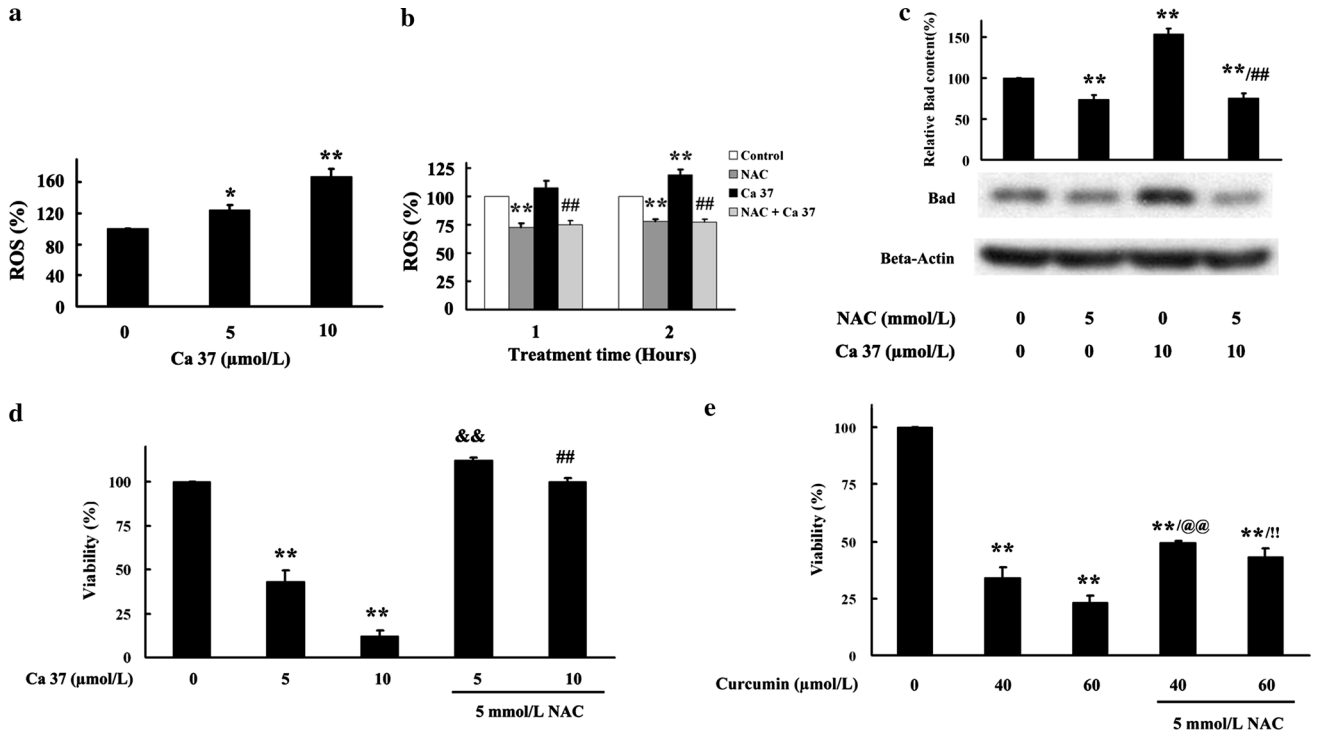

Fig. 4 Reactive oxygen species (ROS) is involved in Ca 37 induced growth inhibition in prostate cancer PC-3 cells. **a** Increased ROS production in PC-3 cells with Ca 37 treatment; **b** NAC abrogated time-dependent ROS production in 10 μmol/L Ca 37-treated PC-3 cells; **c** NAC abrogated Bad expression in PC-3 cells treated with 10 μmol/L Ca 37 for 4 h: the lower panel presents a representative blot and the upper panel presents the semi-quantified statistics normalized with β-actin; NAC prevented growth inhibition of PC-3 cells induced by Ca 37 (**d**) and curcumin (**e**). $^{*}p < 0.05$, $^{**}p < 0.01$ vs. vehicle group; $^{\&\&}p < 0.01$ vs. 5 μmol/L Ca 37 treatment group; $^{\#\#}p < 0.01$ vs. 10 μmol/L Ca 37 treatment group; $^{@@}p < 0.01$ vs. 40 μmol/L curcumin treatment group; $^{!!}p < 0.01$ vs. 60 μmol/L curcumin treatment group. All data were from at least three independent repeat experiments

(110 mg/kg body weight) every other day for 16 days. Tumor growth was determined by caliper measurement of the length (L) and width (W) every 4 days, and tumor volume was calculated on the basis of the following formula: volume $= 0.52 \times L \times W^2$. The body weights of the mice were measured every 4 days during the 16-day treatment period. At the end of study, the tumors were excised, weighed and then lysed for western blot analysis.

Western blot analysis

The cells or tumors were treated with extraction buffer from Beyotime Biotechnology (Haimen, Jiangsu, China) and centrifugated at 17,000*g* for 15 min at 4 °C. The supernatants were collected, and the protein concentrations were determined using a BCA™ Protein Assay Kit. Aliquots containing approximately 20 μg of protein were subjected to SDS polyacrylamide gel electrophoresis and then electroblotted onto nitrocellulose membranes (Millipore). After being blocked with 5 % nonfat milk in TBST, the membranes were incubated with primary antibodies at 4 °C overnight. After washing away the un-combined primary antibodies with TBST, the membranes were incubated with appropriate secondary antibodies for 1 h at room temperature. The western blots were developed using an Enhanced Chemiluminescence Kit (Millipore).

Statistical analysis

All assays were conducted with at least three independent experiments. Data are presented as the mean ± SEM. The statistical significance was evaluated by one-way analysis of variance (ANOVA), followed by Fisher's LSD test. All analyses were performed using the IBM SPSS Statistics software. Significant differences are indicated as follows: $^{*}p < 0.05$, $^{**}p < 0.01$.

Results

The curcumin analogue Ca 37 exhibits potential inhibitory effects in human androgen-independent prostate cancer cells

Compared with curcumin, Ca 37 significantly suppresses the proliferation of human androgen-independent prostate

cancer PC-3 and DU145 cells in a dose-dependent manner within a 24 h period. The IC_{50} value of Ca 37 was 4.7 or 10.5 μmol/L, a value seven or threefold lower than that of curcumin (IC_{50}, 33.8 or 34.3 μmol/L), in PC-3 cells (Fig. 2a1, a2) or DU145 cells (Fig. 2b1, b2), respectively. Ca 37 also exhibited greater inhibitory capacity against prostate cancer PC-3 or DU145 cell migration in scratch-wound assays (Fig. 2c). The bioenergetics system, including the mitochondrial fractions (mitochondrial respiration chain complex enzymes (Complex I to Complex IV) and citric acid cycle enzymes (MDH and α-KGDH activities)) (Fig. 2d1) and cytoplasmic fractions (LDH activity, LA content) (Fig. 2d2), was reduced in Ca 37-treated PC-3 cells. After 8 h treatment with Ca 37, the cell percentage in the G2 phase increased with corresponding decrease in the G1 phase of PC-3 cells (Fig. 2e), indicating that the cells were arrested in G2 phase. There were significant increases in the pro-apoptotic proteins Bad, Bak, activated PARP (89-kD fragment) based on statistical analysis results (Fig. 2f), and condensed chromatin in the nuclei (Fig. 2g) in Ca 37-treated PC-3 cells, indicating apoptosis involved.

The curcumin analogue Ca 37 suppresses prostate cancer tumor xenograft growth in vivo

To determine whether the growth inhibition potential of Ca 37 in vitro could be achieved in vivo, we examined the ability of Ca 37 to suppress the growth of human prostate cancer PC-3 cell xenografts in nude mice. There was a significant inhibition of the growth of the tumor xenografts when mice were treated with 0.5 μmol Ca 37 (Fig. 3a), but not when treated with 6 μmol curcumin (Fig. 3d), which is similar to previous results obtained by Khor et al. [22]. The weights of the excised tumors from the Ca 37-treated mice ranged from 140 to 300 mg, whereas those from the vehicle group ranged from 220 to 480 mg (Fig. 3c). The effects of the compounds on body weight are shown in Figs. 3b, e. There was an increase in the expression of cyclins (Cyclin E and D1) regulating G1/S transition but a decrease in Cyclin A and Cyclin B1, which regulate S/G2 transition and G2/M phase transition, respectively (Fig. 3f). The aberrant expression of cyclins indicates that Ca 37 promotes cancer cells entrance into the cell cycle

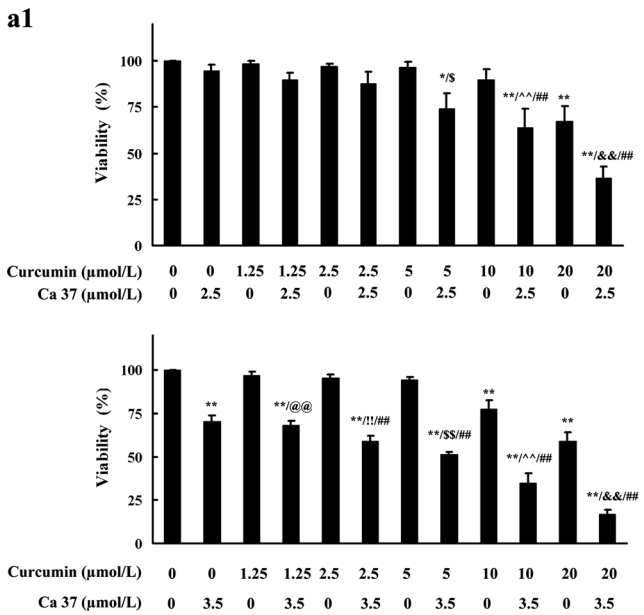

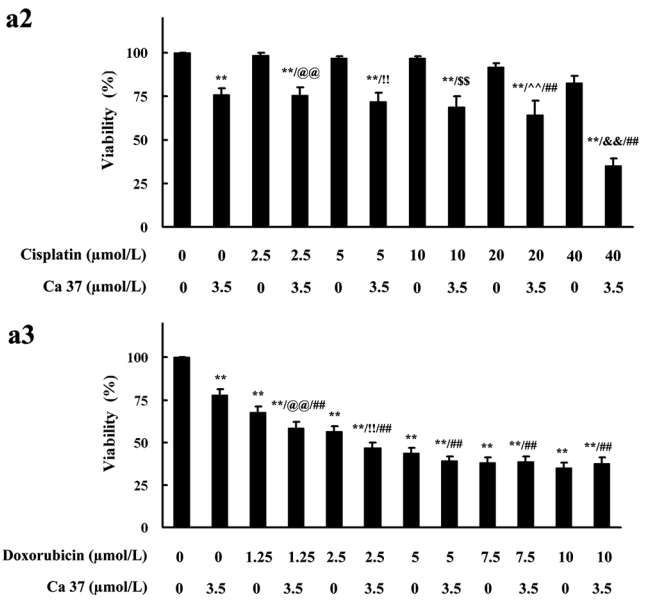

Fig. 5 Ca 37 enhances curcumin induced growth inhibition of prostate cancer cell. The viabilities of cells treated with combinations of curcumin and Ca 37 (**a1**, **b1**), cisplatin and Ca 37 (**a2**, **b2**), doxorubicin and Ca 37 (**a3**, **b3**) for 24 h in **a** PC-3 cells and **b** DU145 cells. **a1** $^{*}p < 0.05$, $^{**}p < 0.01$ vs. vehicle group; $^{\#\#}p < 0.01$ vs. Ca 37 group; $^{@@}p < 0.01$ vs. 1.25 μmol/L curcumin group; $^{!!}p < 0.01$ vs. 2.5 μmol/L curcumin group; $^{\$}p < 0.05$, $^{\$\$}p < 0.01$ vs. 5 μmol/L curcumin group; $^{\wedge\wedge}p < 0.01$ vs. 10 μmol/L curcumin group; $^{\&\&}p < 0.01$ vs. 20 μmol/L curcumin group; **a2** $^{**}p < 0.01$ vs. vehicle group, $^{\#\#}p < 0.01$ vs. Ca 37 group, $^{@@}p < 0.01$ vs. 2.5 μmol/L cisplatin group, $^{!!}p < 0.01$ vs. 5 μmol/L cisplatin group, $^{\$\$}p < 0.01$ vs. 10 μmol/L cisplatin group, $^{\wedge\wedge}p < 0.01$ vs. 20 μmol/L cisplatin group, $^{\&\&}p < 0.01$ vs. 40 μmol/L cisplatin group. **a3** $^{**}p < 0.01$ vs. vehicle group, $^{\#\#}p < 0.01$ vs. Ca 37 group, $^{@@}p < 0.01$ vs. 1.25 μmol/L doxorubicin group, $^{!!}p < 0.01$ vs. 2.5 μmol/L doxorubicin group; **b1** $^{*}p < 0.05$ $^{**}p < 0.01$ vs. vehicle group, $^{\#\#}p < 0.01$ vs. Ca 37 group, $^{\$\$}p < 0.01$ vs. 5 μmol/L curcumin group, $^{\wedge\wedge}p < 0.01$ vs. 10 μmol/L curcumin group, $^{\&\&}p < 0.01$ vs. 20 μmol/L curcumin group; **b2** $^{**}p < 0.01$ vs. vehicle group, $^{\#\#}p < 0.01$ vs. Ca 37 group; **b3** $^{*}p < 0.05$, $^{**}p < 0.01$ vs. vehicle group, $^{\#\#}p < 0.01$ vs. Ca 37 group; **c** Ca 37 enhanced curcumin-induced Bad expression and cleavage of PARP in PC-3 and DU145 cells; **d** NAC partially prevented growth inhibition of PC-3 cells induced by a combination of 10 μmol/L curcumin and 2.5 μmol/L Ca 37 following 24 h of treatment: $^{**}p < 0.01$ vs. vehicle group, $^{\#\#}p < 0.01$ vs. the combination treatment group. All data were from at least three independent repeat experiments

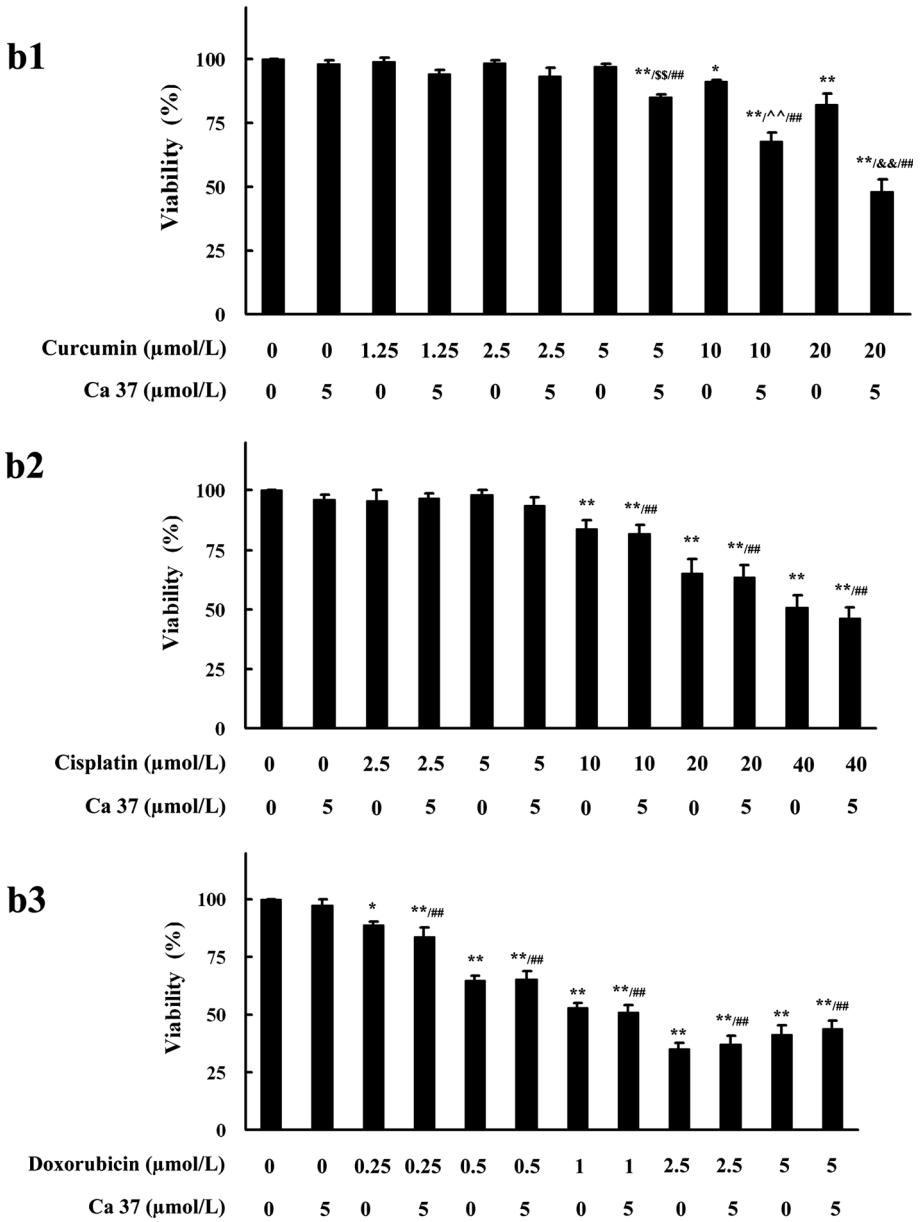

Fig. 5 continued

arrest, which is in accordance with the in vitro result (Fig. 2e).

Reactive oxygen species (ROS) is involved in Ca 37-induced growth inhibition in prostate cancer PC-3 cells

The results of the present study indicated that exposure of PC-3 cells to Ca 37 for 12 h resulted in the generation of ROS (Fig. 4a) and that *N*-Acetyl-cysteine (NAC) abrogated time-dependent ROS production (Fig. 4b). Moreover, NAC prevented Ca 37-induced Bad increase (Fig. 4c). NAC significantly prevented growth inhibition of PC-3 cells induced by Ca 37 but only partially protected cells from the reduced viability induced by curcumin (Fig. 4d, e). These results indicate a different cell death-promoting mechanism induced by curcumin and Ca 37 in PC-3 cells.

Ca 37 enhances curcumin-induced growth inhibition of prostate cancer cells

The treatment of PC-3 cells with Ca 37 (2.5 or 3.5 μmol/L) and increasing doses of curcumin (1.25–20 μmol/L) for 24 h resulted in a dose-dependent inhibition of cell growth (Fig. 5a1). Moreover, the treatment of DU145 cells with Ca 37 (5 μmol/L) and increasing doses of curcumin

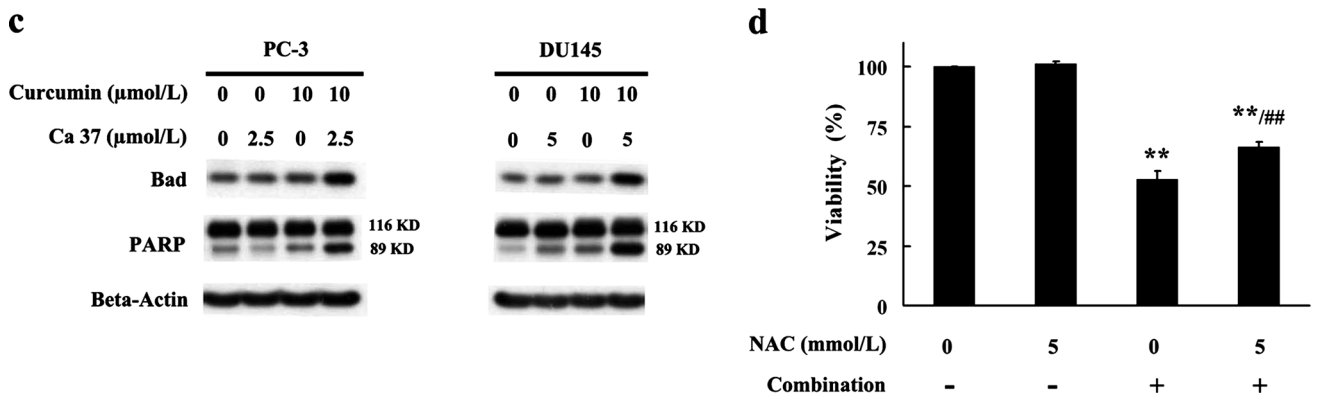

Fig. 5 continued

(1.25–20 μmol/L) for 24 h also resulted in a dose-dependent inhibition of cell growth (Fig. 5b1). Those combination treatments resulted in a more effective inhibition than that of single-compound treatment. The additive effects of the combination of Ca 37 and curcumin suggest a possible synergism (combination index (CI) = 0.93 < 1 for 2.5 μmol/L Ca 37 and 20 μmol/L curcumin in PC-3 cells, CI = 0.96 < 1 for 5 μmol/L Ca 37 and 20 μmol/L curcumin in DU145 cells). However, only a small enhancement of the inhibitory effect was found in the combinations of Ca 37 and high doses of cisplatin (20, 40 μmol/L) (Fig. 5a2) but not with the combination of Ca 37 and doxorubicin (Fig. 5a3) in PC-3 cells. Furthermore, there were no additive effects associated with combinations of Ca 37 and cisplatin (Fig. 5b2) or doxorubicin (Fig. 5b3) in DU145 cells.

We evaluated several factors affecting cell growth to understand the molecular basis of the synergism or additive effects of combination. The combination of Ca 37 and curcumin induced an increase in the expression of the pro-apoptotic protein Bad and cleavage of PARP both in PC-3 and DU145 cells (Fig. 5c). However, NAC partially prevented the growth inhibition of PC-3 cells induced by a combination of 2.5 μmol/L Ca 37 and 10 μmol/L curcumin, which suggests that ROS production was partially involved in this process (Fig. 5d).

Discussion

The present study indicates that the novel curcumin analogue Ca 37 possesses great potential as a promising anti-prostate cancer therapeutic agent comparing with curcumin. Prostate cancer occurs mainly above the age of 50 and is a common cause of cancer death in men. As the aging population is increasing, the number of prostate cancer patients is growing accordingly. Generally, the incidence rates of prostate cancer are higher in western developed countries than in eastern developing countries due to the differences in diet and lifestyle between developed and developing countries [23–25]. Curcumin, a major yellow pigment in turmeric, can suppress prostate cancer cell growth in vitro and in vivo by regulating multiple signaling pathways, including inflammation, cell proliferation, cell motility, and apoptosis [2]. However, studies reveal that serum and tissue levels of curcumin are very low due to poor absorption, rapid metabolism and elimination in the body, which curtails the bioavailability of curcumin [7]. To improve the bioavailability of curcumin, structural analogues of curcumin have been synthesized and reported to exhibit anti-cancer capacities both in vitro and in vivo [9–11, 26–28]. 1,5-Bis(3-hydroxyphenyl)-1,4-pentadiene-3-one, Ca 37, a novel monocarbonyl analogue of curcumin (Fig. 1), exhibits superior potential inhibitory capacities against prostate cancer cell growth and migration (Fig. 2), suppressive effects against prostate cancer tumor xenograft growth (Fig. 3) comparing with curcumin.

Some monocarbonyl or monoketone analogues of curcumin have been synthesized to improve the anti-cancer capacity of curcumin, such as FLLL11 and FLLL12 [29, 30], B19 [31], and B63 [32]. Similar to Ca 37, a β-diketone moiety deletion exists in those analogues. They possess only one carbonyl or ketone and a central methylene carbon, in addition to a 5-carbon tether length between the aromatic rings (curcumin has a 7-carbon tether). Due to the β-diketone moiety deletion in the analogues, they are more stable in a pH 7.4 solution than curcumin. After oral administration, the analogues exhibits decreased degree and speed of metabolism, and much higher peak concentration and a decrease of clearance in the plasma of healthy rats [33]. These traits may explain why Ca 37 is more effective as an anti-prostate cancer agent than curcumin.

ROS (superoxide, hydroxyl radicals, and hydrogen peroxide) promote oxidative damage, such as protein carbonylation, lipid peroxidation and DNA damage, in biomacromolecules. Meanwhile, a small amount of ROS

act as secondary messengers and mediate various signaling cascades related to cellular proliferation, mutation and genetic instability in cancer cells. ROS might function as double-edged swords in cancer therapeutics through an imbalance between ROS generation and elimination. Cells can resist ROS under a cell-death threshold. Once exceeding the threshold, the cells will die [34]. The ROS levels are higher in prostate cancer cell lines than in normal cell lines, implying that cancer cells may be more vulnerable to ROS than normal cells [35]. The generation of ROS increased in Ca 37-treated PC-3 cells and could be abrogated by the ROS scavenger NAC. Moreover, the viability loss prevented by NAC revealed the involvement of ROS in Ca 37-induced growth inhibition. In comparison, curcumin-induced viability loss was only partially involved in ROS (Fig. 4).

It is an interesting phenomenon that Ca 37 enhances the growth inhibitory effect of curcumin, but not doxorubicin or cisplatin, to prostate cancer cells. In present research, ROS plays a vital role in Ca 37 treated prostate cancers. Doxorubicin and cisplatin are also reported to induce cancer cell death through ROS generation [36, 37]. However, curcumin exhibits therapeutic promise for prostate cancer through various pathways [2], whereas ROS is only partially involved. The combination of two or more different pathways (ROS and others) may explain why Ca 37 enhances the growth inhibitory effect of curcumin. It is a hint for us to pay attention to the synergy between structural analogues with different mechanisms but similar biological effects.

In conclusion, the curcumin analogue Ca 37 suppresses both the proliferation of prostate cancer cells in vitro and prostate cancer tumor xenograft growth. In addition, Ca 37 enhances the inhibitory growth effects of curcumin. ROS induction is involved in preferential toxicity of Ca 37 toward prostate cancer cells. Moreover, cell cycle arrest mediated Ca 37-induced tumor cell growth inhibition in vitro and in vivo. Therefore, we believe that Ca 37 has the potential to be used as an anti-cancer candidate for prostate cancer therapy.

Acknowledgments This study was partially supported by the National Natural Science Foundation of China, Key Program 30930105, Foundation of Xi'an Jiaotong University, New Century Excellent Talents in University, the National Natural Science Foundation of China (Grant No. 31070740), and the 985 and 211 Projects of Xi'an Jiaotong University.

References

1. Siegel R, Naishadham D, Jemal A (2012) Cancer statistics, 2012. CA Cancer J Clin 62(1):10–29
2. Teiten MH, Gaascht F, Eifes S, Dicato M, Diederich M (2010) Chemopreventive potential of curcumin in prostate cancer. Genes Nutr 5(1):61–74
3. Fesik SW (2005) Promoting apoptosis as a strategy for cancer drug discovery. Nat Rev Cancer 5(11):876–885
4. Ryter SW, Kim HP, Hoetzel A, Park JW, Nakahira K, Wang X, Choi AM (2007) Mechanisms of cell death in oxidative stress. Antioxid Redox Signal 9(1):49–89
5. Shankar S, Srivastava RK (2007) Involvement of Bcl-2 family members, phosphatidylinositol 3′-kinase/AKT and mitochondrial p53 in curcumin (diferulolylmethane)-induced apoptosis in prostate cancer. Int J Oncol 30(4):905–918
6. Hilchie AL, Furlong SJ, Sutton K, Richardson A, Robichaud MR, Giacomantonio CA, Ridgway ND, Hoskin DW (2010) Curcumin-induced apoptosis in PC3 prostate carcinoma cells is caspase-independent and involves cellular ceramide accumulation and damage to mitochondria. Nutr Cancer 62(3):379–389
7. Anand P, Kunnumakkara AB, Newman RA, Aggarwal BB (2007) Bioavailability of curcumin: problems and promises. Mol Pharm 4(6):807–818
8. Agrawal DK, Mishra PK (2010) Curcumin and its analogues: potential anticancer agents. Med Res Rev 30(5):818–860
9. Lee JW, Hong HM, Kwon DD, Pae HO, Jeong HJ (2010) Dimethoxycurcumin, a structural analogue of curcumin, induces apoptosis in human renal carcinoma caki cells through the production of reactive oxygen species, the release of cytochrome C, and the activation of caspase-3. Korean J Urol 51(12):870–878
10. Wu CL, Liao YF, Hung YC, Lu KH, Hung HC, Liu GY (2011) Ornithine decarboxylase prevents dibenzoylmethane-induced apoptosis through repressing reactive oxygen species generation. J Biochem Mol Toxicol 25(5):312–319
11. Fajardo AM, MacKenzie DA, Ji M, Deck LM, Vander Jagt DL, Thompson TA, Bisoffi M (2012) The curcumin analog ca27 down-regulates androgen receptor through an oxidative stress mediated mechanism in human prostate cancer cells. Prostate 72(6):612–625
12. Weber WM, Hunsaker LA, Abcouwer SF, Deck LM, Vander Jagt DL (2005) Anti-oxidant activities of curcumin and related enones. Bioorg Med Chem 13(11):3811–3820
13. Adams BK, Ferstl EM, Davis MC, Herold M, Kurtkaya S, Camalier RF, Hollingshead MG, Kaur G, Sausville EA, Rickles FR, Snyder JP, Liotta DC, Shoji M (2004) Synthesis and biological evaluation of novel curcumin analogs as anti-cancer and anti-angiogenesis agents. Bioorg Med Chem 12(14):3871–3883
14. Saotome K, Morita H, Umeda M (1989) Cytotoxicity test with simplified crystal violet staining method using microtitre plates and its application to injection drugs. Toxicol In Vitro 3(4):317–321
15. Halliwell B, Whiteman M (2004) Measuring reactive species and oxidative damage in vivo and in cell culture: how should you do it and what do the results mean? Br J Pharmacol 142(2):231–255
16. Luo C, Wang X, Long J, Liu J (2006) An NADH-tetrazolium-coupled sensitive assay for malate dehydrogenase in mitochondria and crude tissue homogenates. J Biochem Biophys Methods 68(2):101–111
17. Janssen AJ, Trijbels FJ, Sengers RC, Smeitink JA, van den Heuvel LP, Wintjes LT, Stoltenborg-Hogenkamp BJ, Rodenburg RJ (2007) Spectrophotometric assay for complex I of the respiratory chain in tissue samples and cultured fibroblasts. Clin Chem 53(4):729–734
18. Hatefi Y, Stiggall DL (1978) Preparation and properties of succinate: ubiquinone oxidoreductase (complex II). Methods Enzymol 53:21–27
19. Luo C, Long J, Liu J (2008) An improved spectrophotometric method for a more specific and accurate assay of mitochondrial complex III activity. Clin Chim Acta 395(1–2):38–41
20. Errede B, Kamen MD, Hatefi Y (1978) Preparation and properties of complex IV (ferrocytochrome c: oxygen oxidoreductase EC 1.9.3.1). Methods Enzymol 53:40–47
21. Humphries KM, Szweda LI (1998) Selective inactivation of α-ketoglutarate dehydrogenase and pyruvate dehydrogenase:

reaction of lipoic acid with 4-hydroxy-2-nonenal. Biochemistry 37(45):15835–15841
22. Khor TO, Keum YS, Lin W, Kim JH, Hu R, Shen G, Xu C, Gopalakrishnan A, Reddy B, Zheng X, Conney AH, Kong AN (2006) Combined inhibitory effects of curcumin and phenethyl isothiocyanate on the growth of human PC-3 prostate xenografts in immunodeficient mice. Cancer Res 66(2):613–621
23. Jemal A, Center MM, DeSantis C, Ward EM (2010) Global patterns of cancer incidence and mortality rates and trends. Cancer Epidemiol Biomarkers Prev 19(8):1893–1907
24. Kimura T (2012) East meets West: ethnic differences in prostate cancer epidemiology between East Asians and Caucasians. Chin J Cancer 31(9):421–429
25. Wolk A (2005) Diet, lifestyle and risk of prostate cancer. Acta Oncol 44(3):277–281
26. Liu Y, Fuchs J, Li C, Lin J (2010) IL-6, a risk factor for hepatocellular carcinoma: FLLL32 inhibits IL-6-induced STAT3 phosphorylation in human hepatocellular cancer cells. Cell Cycle 9(17):3423–3427
27. Liu A, Liu Y, Li PK, Li C, Lin J (2011) LLL12 inhibits endogenous and exogenous interleukin-6-induced STAT3 phosphorylation in human pancreatic cancer cells. Anticancer Res 31(6):2029–2035
28. Ball S, Li C, Li PK, Lin J (2011) The small molecule, LLL12, inhibits STAT3 phosphorylation and induces apoptosis in medulloblastoma and glioblastoma cells. PLoS ONE 6(4):e18820
29. Friedman L, Lin L, Ball S, Bekaii-Saab T, Fuchs J, Li PK, Li C, Lin J (2009) Curcumin analogues exhibit enhanced growth suppressive activity in human pancreatic cancer cells. Anticancer Drug 20(6):444–449
30. Lin L, Hutzen B, Ball S, Foust E, Sobo M, Deangelis S, Pandit B, Friedman L, Li C, Li PK, Fuchs J, Lin J (2009) New curcumin analogues exhibit enhanced growth-suppressive activity and inhibit AKT and signal transducer and activator of transcription 3 phosphorylation in breast and prostate cancer cells. Cancer Sci 100(9):1719–1727
31. Wang Y, Xiao J, Zhou H, Yang S, Wu X, Jiang C, Zhao Y, Liang D, Li X, Liang G (2011) A novel monocarbonyl analogue of curcumin, (1E,4E)-1,5-bis(2,3-dimethoxyphenyl)penta-1,4-dien-3-one, induced cancer cell H460 apoptosis via activation of endoplasmic reticulum stress signaling pathway. J Med Chem 54(11):3768–3778
32. Xiao J, Wang Y, Peng J, Guo L, Hu J, Cao M, Zhang X, Zhang H, Wang Z, Li X, Yang S, Yang H, Liang G (2012) A synthetic compound, 1,5-bis(2-methoxyphenyl)penta- 1,4-dien-3-one (B63), induces apoptosis and activates endoplasmic reticulum stress in non-small cell lung cancer cells. Int J Cancer 131(6):1455–1465
33. Liang G, Shao L, Wang Y, Zhao C, Chu Y, Xiao J, Zhao Y, Li X, Yang S (2009) Exploration and synthesis of curcumin analogues with improved structural stability both in vitro and in vivo as cytotoxic agents. Bioorg Med Chem 17(6):2623–2631
34. Trachootham D, Alexandre J, Huang P (2009) Targeting cancer cells by ROS-mediated mechanisms: a radical therapeutic approach? Nat Rev Drug Discov 8(7):579–591
35. Kumar B, Koul S, Khandrika L, Meacham RB, Koul HK (2008) Oxidative stress is inherent in prostate cancer cells and is required for aggressive phenotype. Cancer Res 68(6):1777–1785
36. Wagner BA, Evig CB, Reszka KJ, Buettner GR, Burns CP (2005) Doxorubicin increases intracellular hydrogen peroxide in PC3 prostate cancer cells. Arch Biochem Biophys 440(2):181–190
37. Miyajima A, Nakashima J, Yoshioka K, Tachibana M, Tazaki H, Murai M (1997) Role of reactive oxygen species in cis-dichlorodiammineplatinum-induced cytotoxicity on bladder cancer cells. Br J Cancer 76(2):206–210